JOURNAL OF MATERIALS SCIENCE 27 (1992) 5609–5691

Effects of thermal history on crystal structure of poly(phenylene sulphide)

J. S. CHUNG*, J. BODZIUCH, P. CEBE
Department of Materials Science and Engineering, Massachusetts Institute of Technology, Cambridge, MA 02139, USA

The lattice parameters of film-grade poly(phenylene sulphide), PPS, have been studied at room temperature as a function of thermal history. Effects of crystallization temperature and annealing time for films crystallized from the rubbery amorphous state were investigated using wide- and small-angle X-ray diffraction, bulk density and thermal analysis techniques. The dimensions of the crystal lattice are found to depend upon prior thermal treatment conditions. As the cold crystallization temperature, T_c, increases, or the annealing time at fixed temperature increases, the bulk density, degree of crystallinity, and crystal perfection increase. With an increase in annealing time at fixed temperature, lattice *a*, *b*, and *c* decrease leading to an increase in lattice density. As the cold crystallization temperature increases, lattice density also increases as a result of a systematic decrease in lattice parameters *a* and *b*.

1. Introduction

The crystalline structure of poly(*p*-phenylene sulphide) (PPS) was first investigated in 1971. Tabor *et al.* [1] reported the crystalline structure of drawn PPS film of Ryton polymer. On the basis of their X-ray studies, they found that the unit cell of PPS has an orthorhombic crystal structure with $a = 0.867$ nm, $b = 0.561$ nm and $c = 1.026$ nm. Brady [2] reported the crystallinity of annealed PPS and its effect on the mechanical properties. By using electron diffraction technique on single-crystal-like lamellae of melt crystallized PPS, Lovinger *et al.* [3] found agreement with the unit cell structure and parameters of Ryton as reported by Tabor *et al.* However, by measuring the crystal structure of small model molecules of PPS, such as 1,4-*bis*(phenylthio)benzene [4] and *bis*-(4-mercaptophenyl) sulphide [5], Garbarczyk [6] suggested that the C–S–C angle of 110 °C in PPS determined by Tabor [1] is too large and should lie within the range of 103°–107°. The smaller C–S–C angle in PPS suggested by Garbarczyk results in a smaller unit cell parameter, *c*, which is in the range 0.980–1.007 nm.

The crystal lattice structure of semicrystalline polymers is strongly related to the kinetic process of crystallization. Therefore, the unit cell parameters should be a function of the crystallization temperature and annealing time. Until the present work, no studies of this kind have been reported on PPS. However, Wakelyn [7] and Hay *et al.* [8] have studied the effect of annealing temperature on the unit cell parameters of another high-performance engineering polymer, poly(etheretherketone), PEEK. Their results indicated an increase in crystal density of cold crystallized PEEK sample with increase in annealing temperature. Increase in crystal density suggests a more dense packing of molecular chains in samples which had experienced higher annealing temperatures. In this work we report the time and temperature dependence of the unit cell parameters of PPS cold crystallized from the rubbery amorphous state.

2. Experimental procedure

Experimental amorphous PPS films, 76.0 μm thick, were used. Information provided by the supplier (Phillips) indicates that these films were made from a medium molecular weight ($M_w = 60\,000$) lightly branched material. Single-crystal mats were made from Ryton V-1 powder and also used for the X-ray study. The preparation method of the single crystal mats has been reported elsewhere [9]. The cold crystallization was performed through direct heating of the PPS amorphous film sample to a desired temperature. The crystallization proceeded from the rubbery amorphous state without melting. A residence time of 1 h was used for cold crystallization temperature studies, and a crystallization temperature of 245 °C was used for studying the annealing time effect on structure. All of the sample preparation was done in a Mettler hot stage under nitrogen gas protection. The melting behaviour of cold crystallized or annealed PPS samples was studied using a Perkin–Elmer differential scanning calorimeter (DSC) model 4 equipped with a thermal analysis data station (TADS). A sample mass of ~ 3 mg and a scan rate of 20 °C min^{-1} were used throughout the entire investigation. Melting peak temperature and heat of fusion were calibrated using an Indium standard.

---

* *Present address*: Engineering Plastics Division, Allied Signal Corporation, Morristown, NJ 07962, USA.

Wide-angle X-ray scattering (WAXS) data were obtained at room temperature using a Rigaku RU-300 X-ray diffractometer which was operated at 50 kV and 200 mA, using CuK_α radiation and a diffracted beam graphite monochromator. The annealed PPS flat film sample was mounted on a flat sample holder and was scanned in reflection mode. The diffraction intensity was measured continuously at 2θ scan rate of 1° min^{-1}; the 2θ measurement range was from 10°–60° with a step scan interval of 0.02°. National Institute of Standards and Technology silicon powder was used on the PPS film surface for internal calibration of diffraction angular positions. Small-angle X-ray scattering (SAXS) data were obtained in transmission at room temperature (unless otherwise indicated) using facilities at the Brookhaven National Synchrotron Light Source.

The bulk density of cold crystallized or annealed PPS was measured in an aqueous $CaNO_3$ density gradient column at room temperature. The density range of the density column is from 1.32–1.38 g cm^{-3}. The measured density was calibrated by standard beads with known density. The accuracy of the density measurement is within 0.0002 g cm^{-3}. After immersion, the sample equilibrated in the column within 1 h, and the density was read within 2 h. The water absorption of PPS is negligible in this time period.

3. Results

3.1. Differential scanning calorimetry

The collective melting endotherms of PPS annealed at 245 °C for various times, are shown in Fig. 1a. Plots of the upper, T_{m2}, and lower, T_{m1}, melting peak temperatures versus annealing time at 245 °C are shown in Fig. 1b. As shown in Fig. 1a, a dual melting peak was observed when the annealing time was shorter than 1470 min at 245 °C. For the early annealing times (1 and 5 min) the height of the lower temperature endotherm is smaller than that of the higher temperature endotherm. However, as the annealing time increases, the peak height of T_{m1} increases relative to T_{m2}, until at 240 min annealing time it becomes the dominant peak. Only a single endotherm is observed at the longest annealing time. The relative crystal distribution between the two melting peaks changes with the residence time. The area underneath the upper melting peak decreases and the area underneath the lower melting peak increases as the residence time increases. From Fig. 1b, temperature T_{m2} remains nearly constant regardless of the residence time at 245 °C, but T_{m1} increases as the residence time increases beyond 1 h. Table I lists the melting peak temperatures and heats of fusion of PPS annealed at 245 °C for various times.

In Fig. 2 the results of the crystallization temperature study are shown. Collective endotherms of PPS cold crystallized at various temperatures for 60 min are shown in Fig. 2a, and the corresponding melting peak temperatures versus T_c are shown in Fig. 2b. The summary of the melting peak temperatures and the heats of fusion of PPS cold crystallized for 1 h at various temperatures are shown in Table II. A double melting peak was also observed in all DSC scans as shown in Fig. 2a. However, for temperature less than 255 °C the lower temperature endotherm is related to the crystallization treatment temperature, while at 255 and 265 °C the small low-temperature endotherm is formed from crystallization during cooling. Fig. 2b shows that the upper melting temperature, T_{m2}, is a constant value (about 274 °C) regardless of the treatment temperature, but the lower melting temperature, T_{m1}, increases approximately linearly with the cold crystallization temperature. This parallels results reported by us for cold crystallized Ryton V-1 [10, 11].

3.2. Wide-angle X-ray scattering (WAXS)

A typical WAXS diffractogram of a PPS film sample which was cold crystallized at 245 °C for 60 min is shown in Fig. 3a. A computer-simulated WAXS diffractogram, based on the *d*-spacing reported by Tabor *et al.* [1] from the PPS fibre diffraction pattern, is also shown in Fig. 3. The simulation was generated by assuming that the 2θ value of the full width at half maximum, FWHM, is 0.8° which is the same value as for the FWHM of the strongest peak from the experimental WAXS result. Comparing the resulting WAXS diffractogram from the flat film sample with the simulated WAXS diffractogram, both are very similar with one exception: the (0 0 4) and (0 0 6) reflections are visible in the simulated diffractogram but are very insignificant in our experimental results. This difference in the WAXS diffractogram is due to the geometric difference in the samples used for the two experiments. The *d*-spacing obtained by Tabor *et al.* [1] was from PPS fibre, in which both the polymer chains and the crystals have the tendency to orient with *c*-axis along the fibre direction. Unoriented film was used in this investigation, and the crystals are isotropically distributed inside the cold-crystallized film. Therefore the (0 0 1) diffractions observed in Tabor *et al.*'s result are relatively insignificant in our investigation.

The strongest diffraction peak at 2θ around 20° consists of two unresolved diffraction peaks, (2 0 0) and (1 1 1). Because of the (2 0 0) and (1 1 1) overlap, we could not use this reflection in determining lattice parameters. Nevertheless, we observed systematic changes in FWHM as a function of thermal treatment. These results are shown in Fig. 4a (annealing time study) and b (crystallization temperature study). The FWHM generally decreases as the annealing time at 245 °C increases. As a function of T_c, FWHM is nearly constant up to 200 °C, then decreases as the crystallization temperature increases further.

Three sharp peaks from silicon powder, located at $2\theta = 28.444°$, 47.303° and 56.121° [12], were used to calibrate the 2θ values of the PPS diffraction peaks. The 2θ values of several major diffraction peaks versus annealing time at 245 °C, or cold-crystallization temperature, are summarized in Tables III and IV, respectively. From the WAXS result of the residence time effect on annealing at 245 °C, as shown in Table III, the diffraction angle, 2θ, of six major diffraction peaks, (1 1 0), (2 0 0) and (1 1 1), (1 1 2), (2 1 1), (0 2 0),

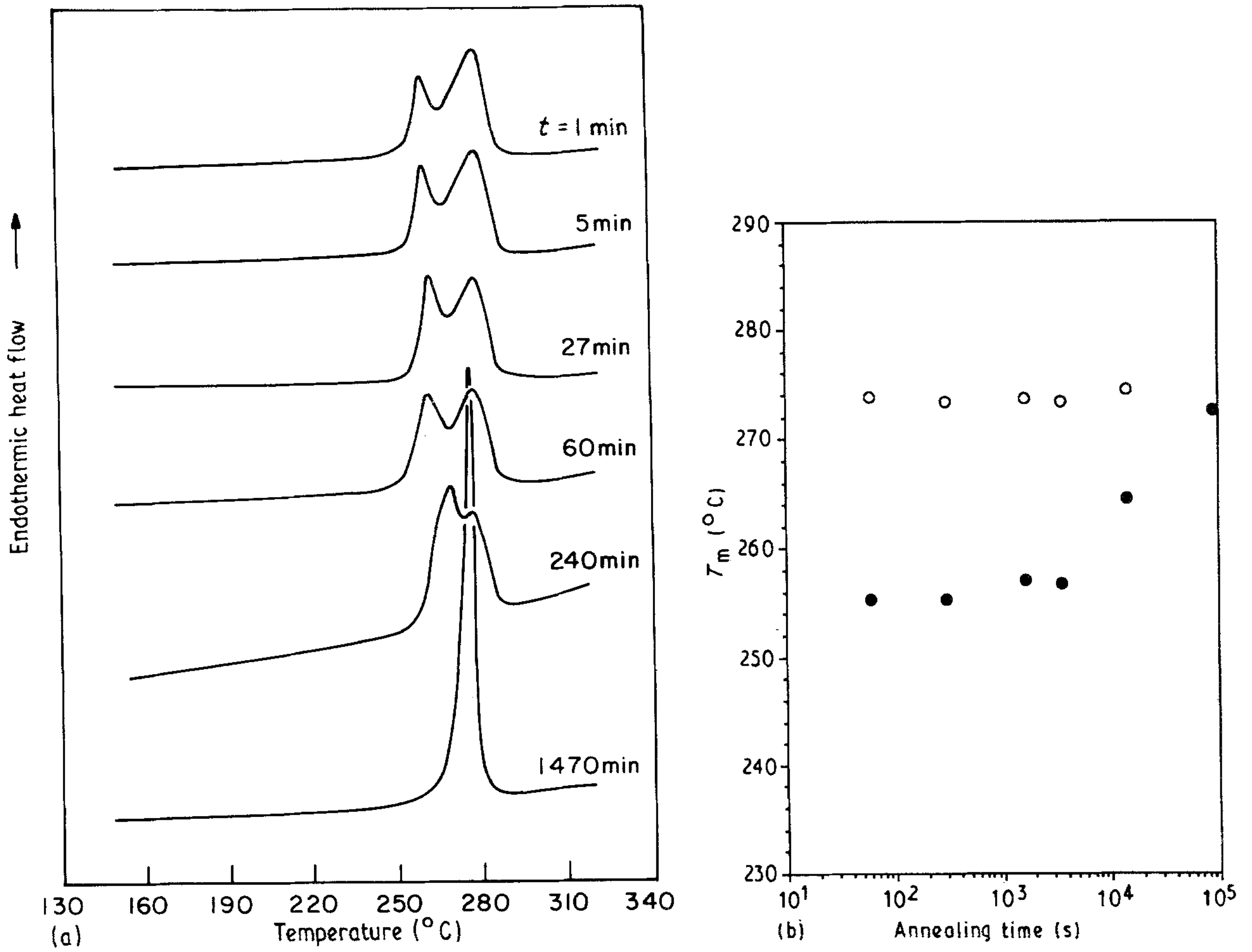

Figure 1 (a) Collective melting endotherms of PPS annealed at 245 °C for the times indicated, $\dot{T} = 20\,°\mathrm{C\,min}^{-1}$. (b) Upper, T_{m2}, (○) and lower, T_{m1}, (●) melting peak temperatures of PPS annealed at 245 °C for the times in (a).

TABLE I Melting peak temperatures, T_{m1} and T_{m2}, and the heat of fusion of PPS cold crystallized at 245 °C for various times

Time (min)	T_{m1}(°C)	T_{m2}(°C)	ΔH(cal g^{-1})
1	255.3	273.9	9.7
5	255.4	273.3	10.0
27	257.0	273.7	10.4
60	256.8	273.4	10.3
240	264.5	274.5	11.0
1470	272.6	–	12.4

and (3 1 1), generally increases as the residence time at 245 °C increases. For the cold-crystallization temperature study, Table IV, the 2θ values of the diffraction peaks increase as the temperature increases up to 245 °C. When the temperature is above 245 °C, nearly all peak positions decrease.

The unit cell dimensions were determined by using an optimized non-linear least squares fitting routine. Five reflections, (1 1 0), (1 1 2), (2 1 1), (0 2 0) and (3 1 1), were used for calculation of unit cell parameters. The plots of the unit cell parameters *a*, *b*, *c* and the density of the PPS crystal versus time of annealing at 245 °C are shown in Fig. 5a–d and are summarized in Table V. In the table, the least certain digits are shown in italics, and are included to show the trends. In the figure, the maximum range of uncertainty is shown by the error bars. When the amorphous films were annealed at 245 °C for various times, we observe a progressive decrease in all unit cell parameters as the annealing time increases, with the smallest relative change occurring in the lattice parameter, *c*. The density of the crystal lattice increases as the annealing process progresses.

Compared to the time-dependent effects for the annealing described above, the relationship of the cold-crystallization temperature and the unit cell parameters is much more complicated. The plots of unit cell parameters and the crystal density versus the cold-crystallization temperature are shown in Fig. 6a–d and are summarized in Table VI. The unit cell parameters *a* and *b* first show a decrease as the cold-crystallization temperature increases, but when the crystallization temperature increases above 245 °C, the unit cell parameters *a* and *b* are variable. The unit cell parameter *c* first increases until reaching the cold-crystallization temperature of 245 °C, then fluctuates. However, the density of PPS crystal increases with crystallization temperature up to 255 °C and decreases when the temperature is 265 °C.

3.3. Bulk density measurement

The plots of bulk density versus log(annealing time) of PPS annealed at 245 °C are shown in Fig. 7a. Bulk density versus crystallization temperature is shown in

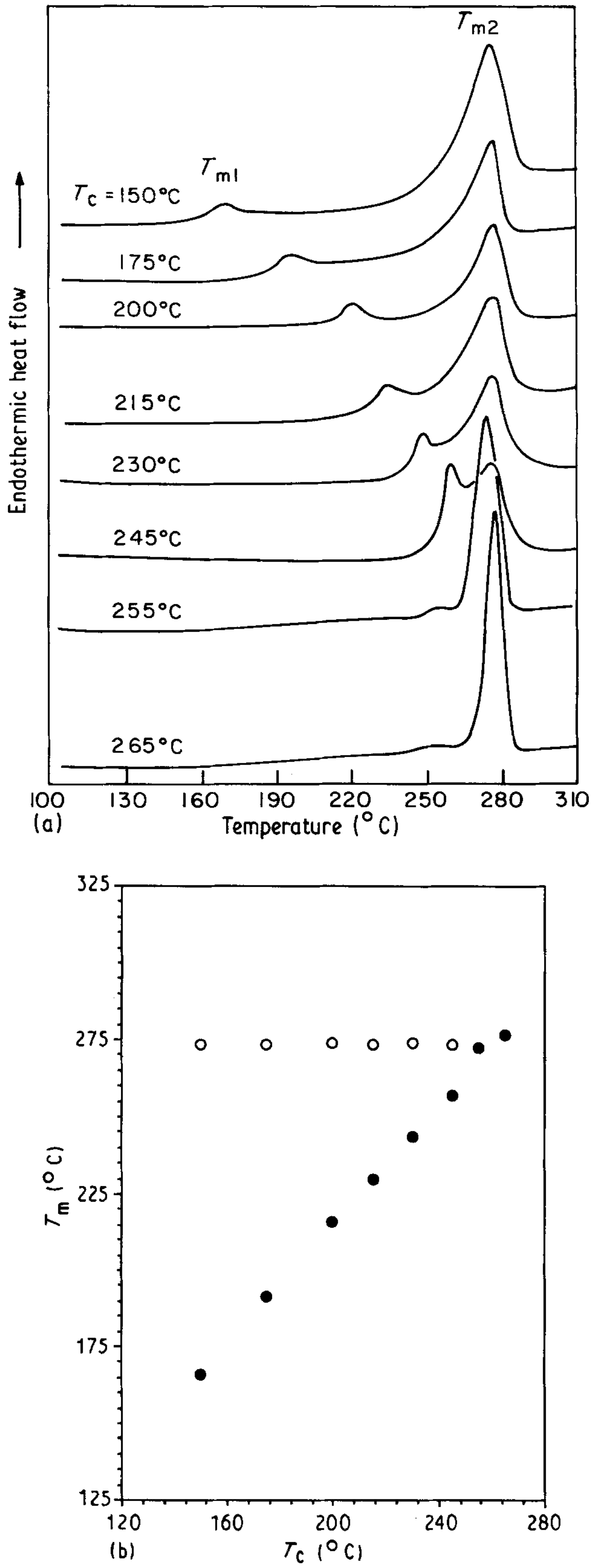

Figure 2 (a) Collective melting endotherms of PPS cold crystallized for 1 h at the indicated temperatures, $\dot{T} = 20\,°\mathrm{C\,min^{-1}}$. (b) Upper, T_{m2}, (○) and lower, T_{m1}, (●) melting peak temperatures of PPS cold crystallized for 1 h at the temperatures in (a).

TABLE II Melting peak temperatures, T_{m1} and T_{m2}, and the heat of fusion of PPS cold crystallized at various temperatures for 1 h

Temperature (°C)	T_{m1}(°C)	T_{m2}(°C)	ΔH(cal g^{-1})
150	166.1	273.5	8.9
175	191.3	273.6	9.5
200	216.0	273.8	9.5
215	230.0	273.3	9.2
230	243.8	274.2	10.0
245	256.7	273.4	10.7
255	272.1	–	11.2
265	276.6	–	11.2

Fig. 7b. The results show that the bulk density of cold-crystallized (or annealed) PPS increases as the crystallization temperature (or annealing time) increases. The bulk density and weight per cent degree of crystallinity were calculated from both density and DSC measurements and are summarized in Table VII (time study), and Table VIII (crystallization temperature study). The degree of crystallinity determined from DSC results, X_c(DSC), was calculated from the endotherm area based on our new value for the heat of fusion of 100% crystalline PPS [13], $\Delta H_f = 112\,\mathrm{J\,g^{-1}}$. The degree of crystallinity determined from bulk density, X_c(den), was calculated from a two-phase model in which both amorphous density and crystal lattice density must be known. The calculation was based on the measured value of $1.319\,\mathrm{g\,cm^{-3}}$ for amorphous PPS. The crystal density value was varied according to each crystallization condition, from lattice density values shown in the last columns of Tables V and VI. X_c(DSC) increases as the annealing time at 245 °C increases, while X_c(den) does not vary regularly with the annealing time. It is likely that the density of the amorphous phase inside the semicrystalline sample varies with crystallization or annealing conditions, just as the crystal lattice density does. However, we are not able to take this change into account in the two-phase model of bulk density. This is one possible reason that the crystallinity calculated from bulk density is so variable. On the other hand, in the crystallization temperature study, the degrees of crystallinity, X_c(DSC) and X_c(den), both generally increase as the cold crystallization temperature increases. Results show that the degree of crystallinity calculated from DSC measurement is about 5%–10% higher than that calculated using a two-phase assumption and the room-temperature density measurement. Although we found that PPS contains a much larger rigid amorphous fraction [13, 14] than that originally reported by Cheng *et al.* [15], we found that the two-phase assumption was still a good model to interpret the density data. The reason for the validity of the two-phase assumption in the density analysis is due to the fact that the additional rigid phase has a density close to that of the mobile amorphous phase [16]. As a function of thermal treatment conditions, both mobile amorphous and rigid amorphous phases may have density variation, which was not taken into account in crystallinity determination.

3.4. Small-angle X-ray scattering

Room-temperature SAXS patterns were recorded for all PPS films. A very broad, shallow maximum was observed at the lowest crystallization temperatures, and the peak became much more distinct as the cold crystallization temperature increased. In the annealing

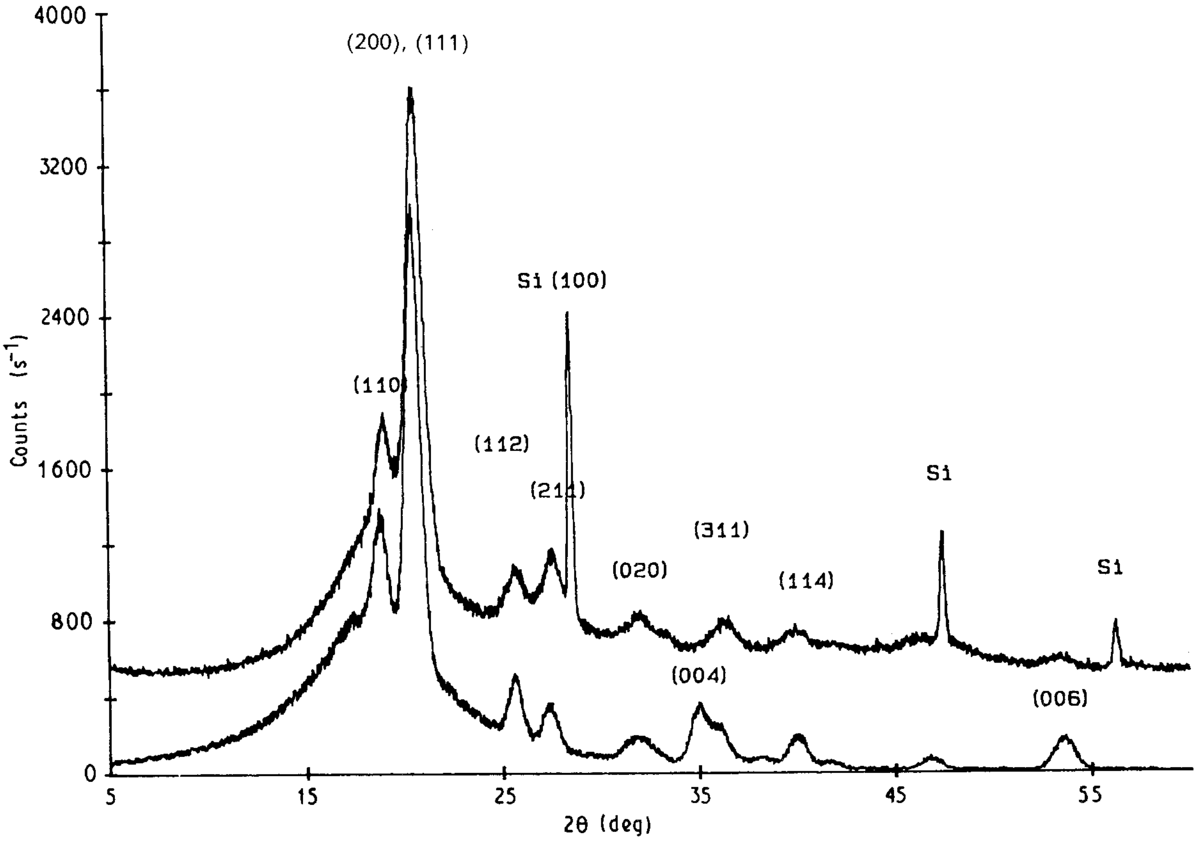

Fogire 3 (a) Wide-angle X-ray diffractogram of PPS film cold crystallized at 245°C for 60 min and (b) simulated diffractogram of PPS fibre from the *d*-spacing reported by Tabor *et al.* [1] showing (004) and (006) peaks.

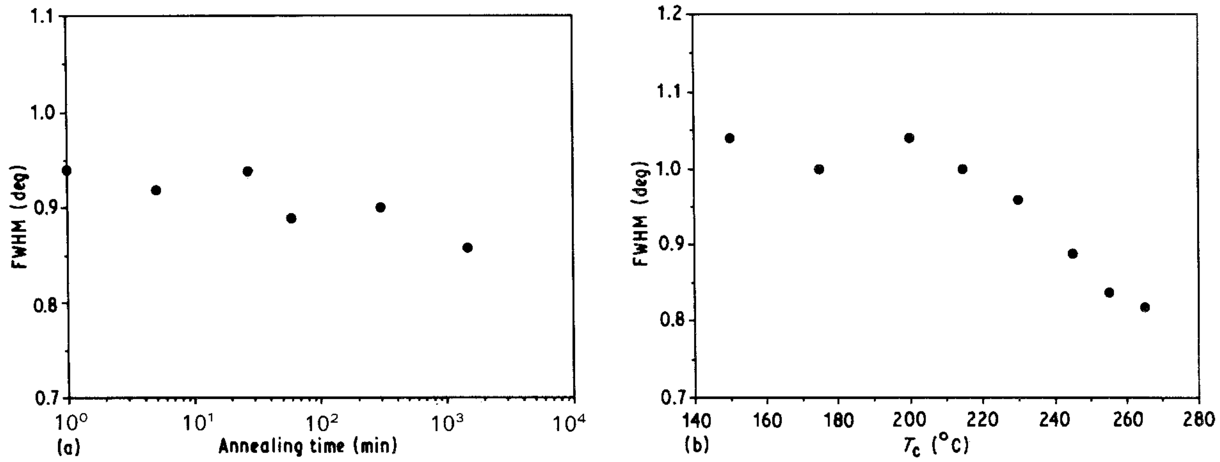

Figure 4 Full width at half maximum, FWHM, of the most intense diffraction peak (overlap of (2 0 0) and (1 1 1)) versus (a) annealing time or (b) cold-crystallization temperature.

TABLE III 2θ values of six major wide-angle X-ray diffraction peaks of PPS annealed at 245 °C for various times

Time (mins)	(1 1 0)	(2 0 0), (1 1 1)	(1 1 2)	(2 1 1)	(0 2 0)	(3 1 1)
1	18.863	20.562	25.565	27.433	31.728	35.155
5	18.931	20.598	25.569	27.441	31.841	36.179
27	18.928	20.603	25.589	27.441	31.843	36.241
60	18.928	20.622	25.639	27.501	31.844	36.261
240	18.949	20.619	25.633	27.485	31.876	36.285
1470	18.970	20.636	25.632	27.499	31.909	36.310

time study, because of the high treatment temperature, a very distinct maximum was observed whose peak position did not change with time. Peak position was analysed by simple application of Bragg's law to obtain the long period, *L*, which is listed in Tables VII (time study) and VIII (temperature study). In Table VII, the long period did not vary with treatment time in a regular manner. All the long periods listed are

TABLE IV 2θ values of six major wide-angle X-ray diffraction peaks of PPS cold crystallized at various temperatures for 1 h

Temperature (°C)	(1 1 0)	(2 0 0), (1 1 1)	(1 1 2)	(2 1 1)	(0 2 0)	(3 1 1)
150	18.701	20.358	25.602	27.229	31.691	35.836
175	18.845	20.460	25.550	27.265	31.723	35.930
200	18.849	20.484	25.569	27.318	31.763	36.078
215	18.861	20.532	25.581	27.368	31.817	36.114
230	18.909	20.544	25.594	27.349	31.862	36.184
245	18.928	20.622	25.639	27.501	31.844	36.261
255	18.928	20.631	25.625	27.501	31.802	36.234
265	18.896	20.604	25.609	27.592	31.862	36.199

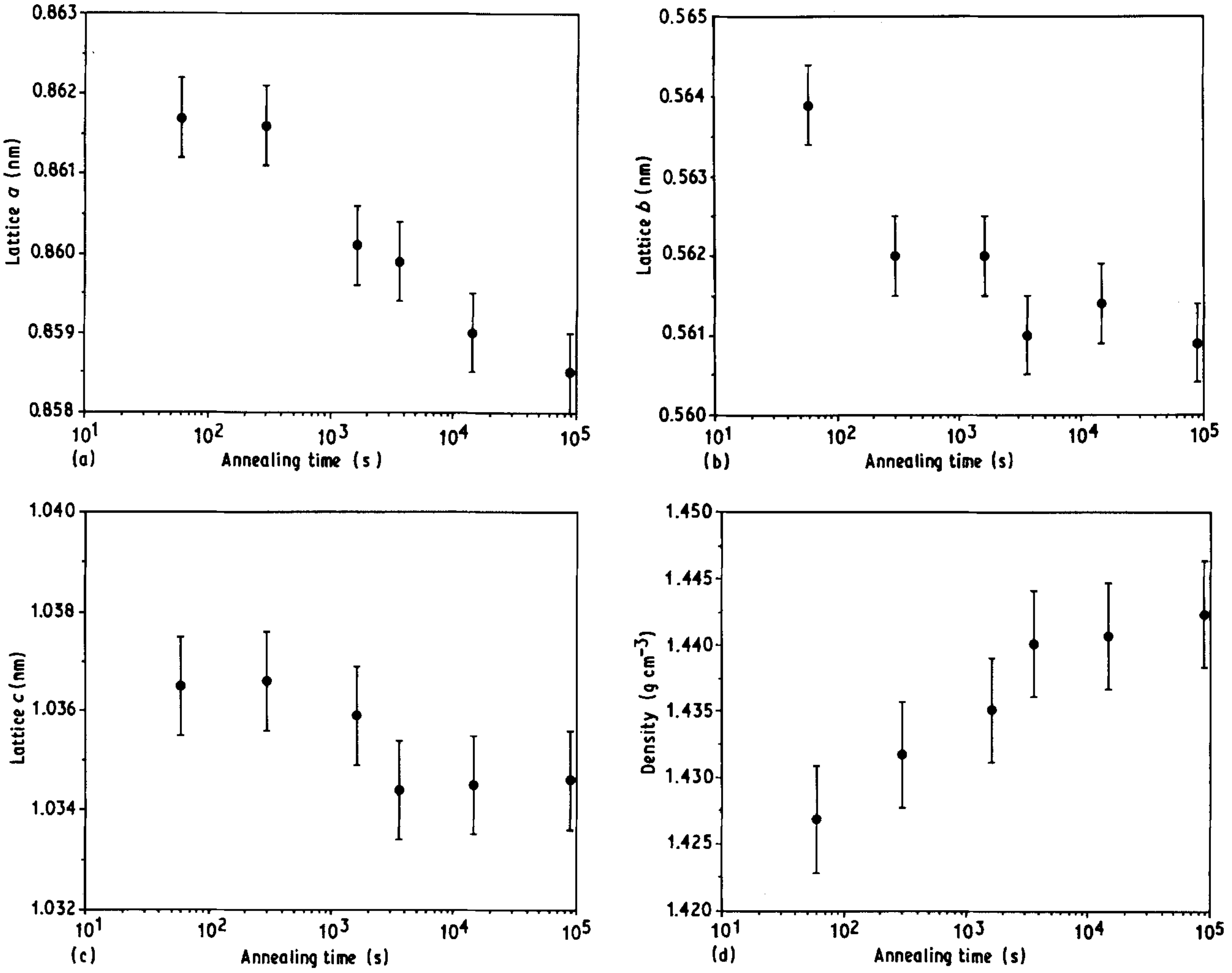

Figure 5 Lattice parameters versus annealing time at 245 °C: (a) unit cell parameter, *a*; (b) unit cell parameter, *b*; (c) unit cell parameter, *c*; (d) lattice density.

TABLE V Unit cell parameters, unit cell volume and lattice density of PPS annealed at 245 °C for various times

Time (min)	*a* (nm)	*b* (nm)	*c* (nm)	Volume (nm^3)	Density (g cm^{-3})
1	0.8617	0.5639	1.0365	0.50265	1.427
5	0.8616	0.5620	1.0366	0.50194	1.432
27	0.8601	0.5620	1.0359	0.50073	1.435
60	0.8599	0.5610	1.0344	0.49900	1.440
240	0.8590	0.5614	1.0345	0.49888	1.440
1470	0.8585	0.5609	1.0346	0.49819	1.442

Maximum experimental error for *a* and *b* is ± 0.0005 nm and for *c* is ± 0.001 nm.

within the experimental error involved in determining the peak positions. As a result of the increase in the degree of crystallinity (using X_c(DSC)) the lamellar thickness, *l*, increases slightly with annealing time. In the crystallization temperature study, Table VIII, the long period increases with T_c in a regular manner, though the change is slight at the lowest crystallization temperatures. The increase over the temperature

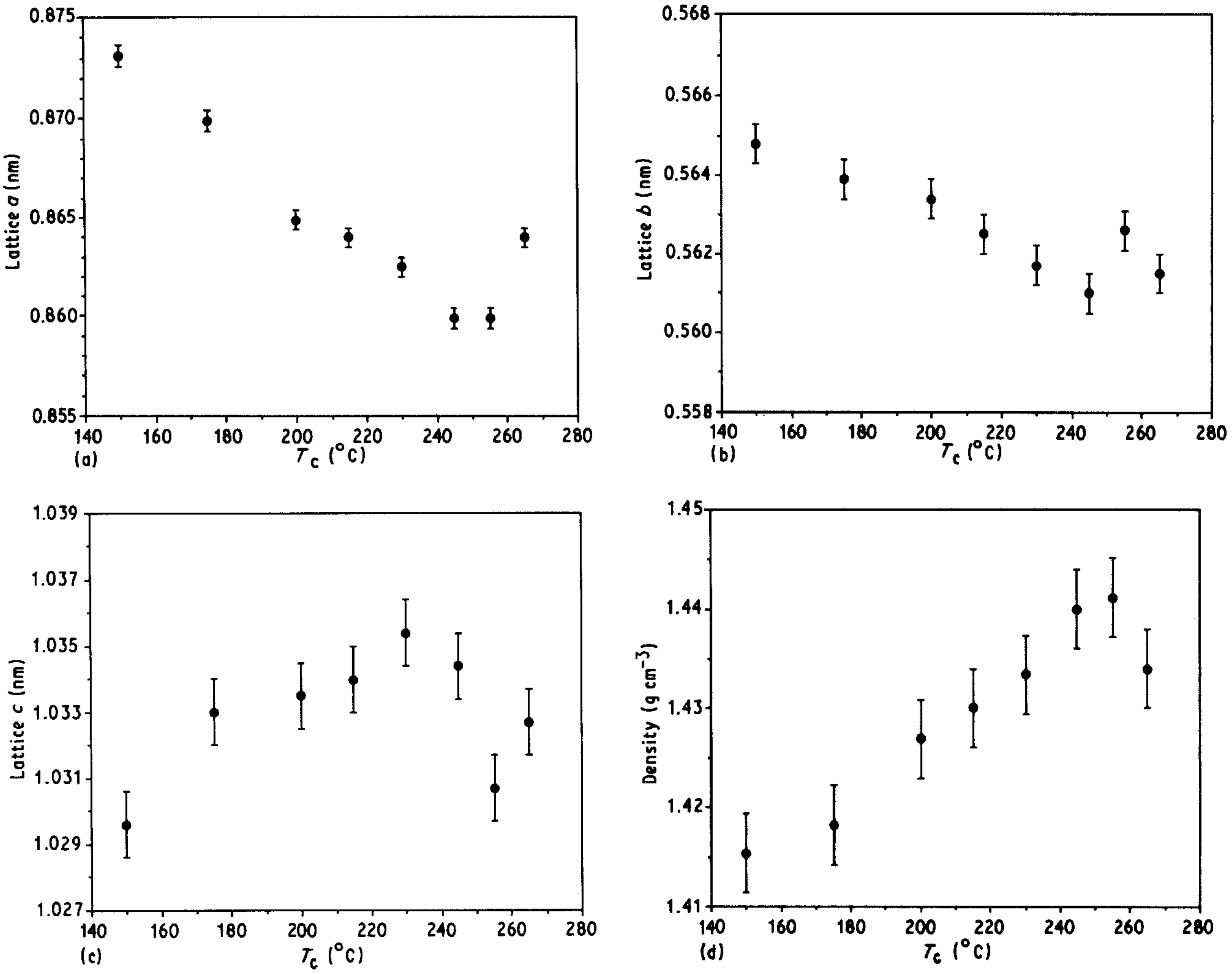

Figure 6 Lattice parameters versus cold-crystallization temperature: (a) unit cell parameter, *a*; (b) unit cell parameter, *b*; (c) unit cell parameter, *c*; (d) lattice density.

TABLE VI Unit cell parameters, unit cell volume and lattice density of PPS cold crystallized at various temperatures for 1 h

Temprature (°C)	*a* (nm)	*b* (nm)	*c* (nm)	volume (nm^3)	Density (g cm^{-3})
150	0.8731	0.5648	1.0296	0.50772	1.415
175	0.8699	0.5639	1.0330	0.50672	1.418
200	0.8649	0.5634	1.0335	0.50361	1.427
215	0.8640	0.5625	1.0340	0.50252	1.430
230	0.8625	0.5617	1.0354	0.50162	1.433
245	0.8599	0.5610	1.0344	0.49900	1.440
255	0.8599	0.5626	1.0307	0.49863	1.441
265	0.8640	0.5615	1.0327	0.50100	1.434

Maximum experimental error for *a* and *b* is ± 0.0005 nm and for *c* is ± 0.001 nm.

range is well outside the limits of our experimental error. The lamellar thickness shows a similar increase. These results are similar to those of Murthy *et al.* [17] performed on oriented, annealed PPS. However, D'Ilario and Piozzi found no trend in long period with crystallization temperature for solution grown crystals [18].

4. Discussion

The unit cell parameters show a strong dependence on thermal history for annealed PPS films, as shown in Fig. 5a–d. The lattice parameters, *a*, *b*, and *c* decrease with annealing time. As a result, the lattice density of annealed PPS increases as the annealing time increases. This indicates that the overall PPS polymer chains packing into the crystalline state become closer (smaller lattice parameters) or more perfect (smaller lattice volume or larger lattice density) as the time of annealing at 245 °C progresses. The largest change occurs in the lattice parameters *a* and *b*, as a result of the relatively weak Van der Waals forces between the polymer chains. In order to study the annealing time effect on the lattice parameters, the lattice parameters are plotted versus 1/(log(annealing time)) and the plots are shown in Fig. 8a–c. We found that the unit cell parameters, *a*, *b* and *c*, increase linearly with the inverse of log(annealing time). By extrapolating to the

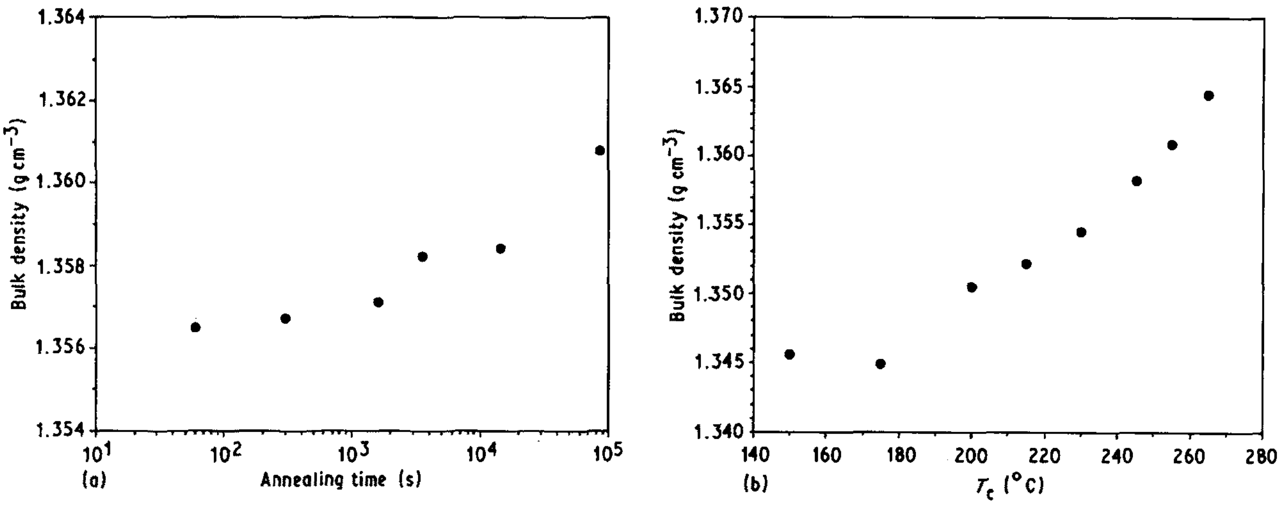

Figure 7 Bulk density versus (a) annealing time at 245 °C, and (b) crystallization temperature.

TABLE VII Bulk density, weight degree of crystallinity, long period, and lamellar thickness of PPS annealed at 245 °C for various times

Time (min)	ρ_b(g cm^{-3})	χ_c(den)[a]	χ_c(DSC)[b]	L(nm)	l(nm)
1	1.3565	0.37	0.37	13.4	5.0
5	1.3567	0.36	0.38	13.4	5.1
27	1.3571	0.35	0.39	–	–
60	1.3582	0.34	0.39	13.6	5.3
240	1.3584	0.34	0.42	14.1	5.9
1470	1.3608	0.36	0.47	13.2	6.2

[a] Weight degree of crystallinity calculated based on the measured density value 1.319 g cm^{-3} for amorphous PPS, and crystal lattice density varied according to each crystallization condition.

[b] Weight degree of crystallinity calculated from the area under the DSC endotherm.

infinite annealing time, the infinite time unit cell parameters, a_0, b_0, and c_0, of cold-crystallized PPS film at 245 °C can be estimated. At infinite annealing time, we find values of $a_0 = 0.857$ nm, $b_0 = 0.559$ nm and $c_0 = 1.033$ nm. This value of the c lattice parameter is larger than that reported for Ryton PPS [1, 3] and is a result of chemical structure differences in the PPS starting material. When we performed similar experiments on Ryton PPS single-crystal mats [10], the c lattice parameter agreed well with other reports. This point will be discussed in more detail later, but the result for lattice c is reproducible, and depends upon starting material. The values of all lattice parameters calculated at infinite annealing time lead to a crystal density of 1.451 g cm^{-3}. Also from Fig. 4a, the FWHM of the annealed PPS decreases as the time of annealing increases. Hence, both crystal density and the crystallite size of the annealed PPS increase as the annealing time increases.

The weight average degree of crystallinity of PPS determined either from DSC or from density measurements has a larger value than reported by White and co-workers [19, 20] and a smaller value than reported by Brady [2]. This is due to the difference in the heat of fusion of the 100% crystalline PPS determined by these groups. Brady's value of heat of fusion, 85 J g^{-1}, was determined from a single datum and therefore has a very large uncertainty [2]. White *et al.* [19, 20] used a series of oriented samples for crystallinity measurement, and obtained a heat of fusion value of 146 J g^{-1}. Based on density, WAXS, and DSC results, Huo and Cebe[13, 16] found the heat of fusion, ΔH_f, for 100% crystalline PPS to be 112 J g^{-1}. We believe that the very large difference between our results and those of White and co-workers [19, 20] is due to differences in the way the heat of melting is measured. We previously determined [10] that there is an exothermic region in between the two endothermic melting peaks when PPS is cold crystallized from the rubbery amorphous state. This exothermic region must be considered in any calculation of heat of fusion. For example, when this exothermic region is taken into account and a proper baseline determined, we find that quenched PPS has a heat of crystallization which is equal to the heat of melting, within experimental error. Quenched PPS is indeed amorphous, as further evinced by a density of 1.319 g cm^{-3}, which is very close to the amorphous density determined by Tabor *et al.* [1]. Cebe and co-workers [10, 14, 16] used the total endothermic area minus the exothermic region between the two endotherms (called the calibrated heat of fusion [10]) in determining the heat of melting of the crystals existing in the sample prior to the DSC scan. They then determined the heat of fusion to be 112 J g^{-1}, for 100% crystalline PPS by extrapolating from plots of the calibrated heat of fusion versus either the specific volume (from density measurement) or the degree of crystallinity (from WAXS). In this work, all crystallinity measurements reported in Tables VII and VIII were made using the calibrated heat of fusion.

The relationship of the unit cell parameters of cold-crystallized PPS with the crystallization temperature is complicated, and depends upon whether crystallization is completed at the chosen temperature. The lattice parameters a and b first decrease then become variable as the temperature increases above 245 °C, as shown in Fig. 6a and b. This is most probably due to the fact that the cold crystallization process is not complete in 1 h, and there is some fraction uncrystallized after this time when the crystallization temperature is over 245 °C. It can be seen in Fig. 2a

TABLE VIII Bulk density, weight degree of crystallinity, long period, and lamellar thickness of PPS cold crystallized at various temperatures for 1 h

Temperature (°C)	ρ_b(g cm^{-3})	χ_c(den)[a]	χ_c(DSC)[b]	L(nm)	l (nm)
150	1.3456	0.31	0.34	11.0	3.7
175	1.3449	0.28	0.36	11.1	4.0
200	1.3505	0.32	0.36	11.4	4.1
215	1.3522	0.32	0.35	11.5	4.0
230	1.3545	0.34	0.38	12.4	4.7
245	1.3582	0.34	0.41	13.4	5.5
255	1.3609	0.36	0.43	–[c]	–[c]
265	1.3645	0.38	0.43	16.0	6.9

[a] Weight degree of crystallinity calculated using the measured density value 1.319 g/cc for amorphous PPS, and crystal lattice density varied according to each crystallization condition.

[b] Weight degree of crystallinity calculated from the area under the DSC endotherm.

[c] Not tested under this condition.

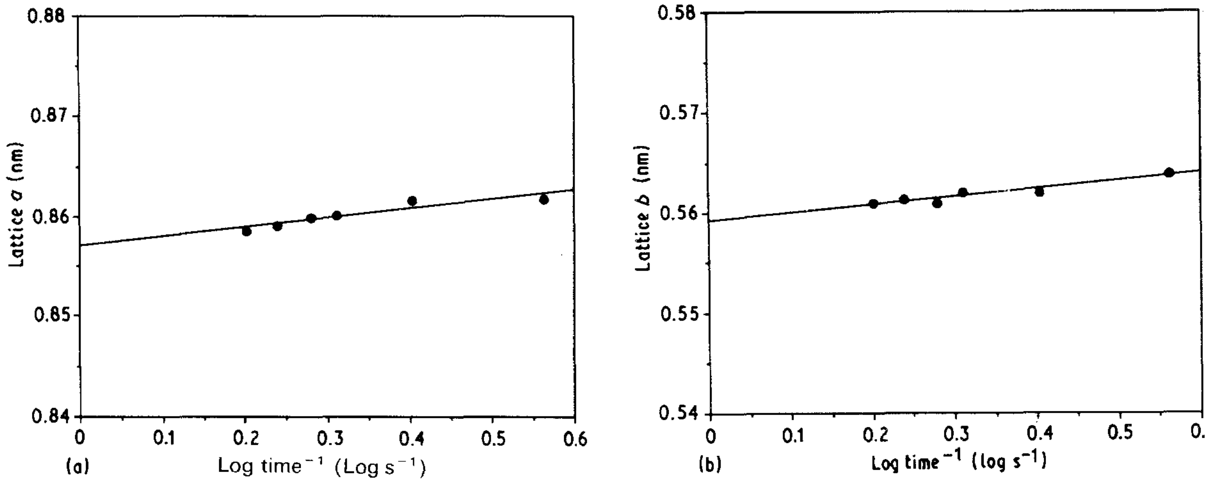

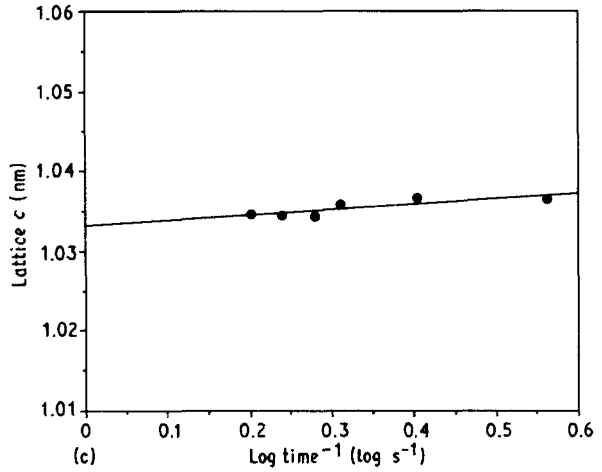

Figure 8 Lattice parameters versus 1/log (annealing time) of PPS annealed at 245 °C: (a) unit cell parameter, *a*; (b) unit cell parameter, *b*; (c): unit cell parameter, *c*.

that a small endothermic peak exists in the DSC thermograms just before the main melting peak for annealing temperatures of 255 and 265 °C. This indicates the formation of crystals during cooling rather than at the cold crystallization temperature. Thus, the data above 245 °C represent the structure which is not equilibrated. In view of the effect of time upon the lattice parameters at fixed crystallization temperature, it is reasonable to suggest that the parameters *a* and *b* determined at 255 and 265 °C are larger than what would be expected if the crystallization time were sufficiently long to result in complete crystallization at T_c.

The lattice parameter *c* shows a variation with the crystallization temperature, seen in Fig. 6c, slightly increasing up to 245 °C and then becoming variable. The effect of thermal treatment on the crystal lattice parameters has not been reported for PPS, but Hay *et al.* [8] and Wakelyn [7] have reported the lattice parameter investigation of another engineering semicrystalline polymer, poly(ether ether ketone), PEEK. Hay *et al.* [8] reported that the unit cell parameter, *c*, of compression-moulded PEEK linearly decreases with annealing temperature, though the dependence on temperature is weak. The unit cell parameter, *c*, reported by Wakelyn [7] on commercial amorphous films of PEEK shows first an increase and then a decrease as the cold-crystallization temperature increases. In our experimental method, the calculation of unit cell parameter, *c*, involves only three sets of angular reflections, therefore the experimental error is bigger (about 0.001 nm) than in the other parameters, *a* and *b*. However, as in the commercial amorphous film of PEEK, the PPS unit cell parameter *c* first increases then decreases as the crystallization temperature increases.

We suggest that the variation in unit cell parameter *c* relates both to the nature of the starting material, which for our study is thin amorphous film (the same type of sample as for Wakelyn's experiments on PEEK) and to the cold crystallization process. During the manufacturing of commercial amorphous film, some degree of molecular orientation exists in the plane of the film. This may affect the initial cold crystallization which occurs from a state of very low molecular mobility. All the temperatures used in this study are above the maximum in the linear growth rate versus temperature curve for PPS [3, 10, 21, 22]. Thus, most crystals nucleate very rapidly at a lower temperature during heating to the cold-crystallization temperature. The cold-crystallization process is really one of further growth and annealing of already nucleated crystals. Only at the very highest crystallization temperatures of 255 and 265 °C (which are only 10–20 °C below the melting point) would we expect that there may be some fraction of crystals melted which cannot crystallize completely.

At the lowest cold-crystallization temperatures, we know from other studies that there is a very large amount of rigid amorphous phase created. It has been suggested that the rigid amorphous phase comprises amorphous material that becomes strained during crystallization [15]. This is supported by the fact that the largest amount of rigid amorphous phase is created during conditions of rapid crystal growth, such as cold crystallization or non-isothermal crystallization at high cooling rate. Based on our new heat of fusion data for PPS [13, 16] the amount of the rigid amorphous phase may be as large as 0.45. As a function of cold-crystallization temperature, the amount of the rigid amorphous phase decreases while the overall degree of crystallinity increases. The increase of crystal thickness and overall degree of crystallinity shown in Table VIII may occur by crystals thickening into regions previously occupied by the rigid amorphous phase. This would be likely to result in strain in the crystals along the lattice *c* direction. While lattice *a* and *b* pack more tightly, and the overall lattice density still increases, the incorporation of rigid amorphous phase material into thickening crystals may lead to the slight increase of lattice parameter *c* as the crystallization temperature increases. As the temperature further increases above 245 °C, all the lattice parameters show an irregular behaviour. Because cold-crystallization time and temperature both affect the lattice parameters, the variability above 245 °C may be the result of the choice of 1 h crystallization time. The 1 h time may be insufficient to allow completion of the crystallization process, as further indicated by the observation of the small endotherm (Fig. 2a) below the main peak due to imperfect crystals formed during cooling. At temperatures lower than 255 °C, 1 h was sufficient to complete the crystallization so that no more crystals formed during cooling.

In this work we have found that the unit cell parameters for PPS depend upon both cold-crystallization time and temperature. The temperature study result shows that as T_c increases there is an increase in the lattice density, which is similar to the result on PEEK polymer [7, 8]. In addition, we find that the lattice parameter *c* depends on the starting material. Results for *a*, *b*, and *c* parameters are compared in Table IX to values previously reported. Our results for cold-crystallized film are expressed in terms of the range of values measured in the present study of the effects of temperature and time. All other studies of PPS lattice parameters treated Ryton V-1 PPS. Choice of starting material has a large effect on the lattice parameter *c*.

Our results indicate that the unit cell parameter *c*, for any treatment condition, is 0.3%–1% higher than reported by Tabor *et al.* [1] and Lovinger *et al.* [3]. This difference of the unit cell parameter *c* is due to the chemical structure differences of the materials used. Low molecular weight Ryton V-1 PPS was used in both prior works [1, 3], but an experimental film made from branched, medium molecular weight PPS was used in this study. The crystallization kinetics and crystalline structure will be affected by the molecular weight, chain branching and entanglement. As we reported in our study of the bulk crystallization rate [10], the crystallization rate of the branched, medium molecular weight film grade PPS is slower than the rate of low molecular weight Ryton V-1 PPS. The degree of crystallinity of cold- or melt-crystallized experimental film sample is about 15% less than that of Ryton V-1 [10, 11] assuming the same heat of fusion, and the upper melting peak temperature of the film grade is about 10 °C lower than that of Ryton V-1. All our results indicate that the crystalline structure of the branched, medium molecular weight film specimen is less perfect compared to that of Ryton V-1 sample under similar crystallization conditions, due to chain

TABLE IX Summary of the published unit cell parameters, unit cell volume and lattice density of melt and cold-crystallized PPS

Materials	*a* (nm)	*b* (nm)	*c* (nm)	Unit cell volume (nm^3)	Density ($g\,cm^{-3}$)	Reference
Cold-crystallized film	8.54–8.73[a]	5.61–5.65[a]	10.30–10.37[a]	493.5–511.5[a]	1.416–1.443[a]	Present
Mat of solution-grown crystals[b]	8.56[c]	5.61	10.17	488.4	1.476	[9]
	8.64[d]	5.62	10.24	497.2	1.442	
Fibre[b]	8.67	5.61	10.26	499.0	1.440	[1]
As-received powder[b]	8.56	5.61	9.80–10.07	468.1–481.0	1.494–1.535	[6]
Melt crystallized film[b]	8.68	5.66	10.26	504.0	1.426	[3]

[a] Range covers all test conditions.
[b] Starting material is Ryton V-1 PPS.
[c] Single-crystal mat grown at 182.5 °C.
[d] Single-crystal mat grown at 172.5 °C.

branching and molecular entanglement effects. Once again the chain branching and molecular entanglement will have the biggest effect in the unit cell parameter *c* direction, because branching and entanglement serve as restraints on chain packing along the chain direction. We have additional evidence to confirm that the value of the *c* lattice parameter depends on the starting material [9]. As shown in Table IX, the unit cell parameters *a* and *b* of our PPS single crystal mats [9] made from Ryton V-1 are the same as other reports on Ryton. The lattice parameter *c* is the same (or slightly smaller) compared to reported results, but is much smaller than the value measured here for the film grade material.

5. Conclusion

We have utilized wide-angle X-ray diffraction to determine the temperature and annealing time dependence of the lattice parameters and lattice density in PPS. Our results show that the dimensions of the PPS unit cell depend upon thermal treatment history in a similar manner to that seen in PEEK polymer [7, 8]. We observed that as the annealing time at fixed temperature increases, the crystal structure becomes more compact: lattice parameters *a*, *b*, and *c* systematically decrease, leading to an increase in lattice density. As the cold crystallization temperature increases, lattice parameters *a* and *b* systematically decrease, while *c* slightly increases. The result is an increase in overall lattice density. Under both treatment conditions we find that the bulk density and degree of crystallinity increase; the long period increases; and the crystallite size increases. Lattice parameter *c* for film grade material is 0.3%–1% larger than for Ryton PPS.

Acknowledgement

The authors acknowledge the Esther and Harold E. Edgerton Fund for support of this research. JSC thanks IBM for a predoctoral fellowship. JB participated in this research through the Undergraduate Research Opportunity Program. A portion of this research was conducted at the Brookhaven National Synchrotron Light Source. The assistance of Dr Alex Darovsky in using the Brookhaven Synchrotron is acknowledged.

References

1. B. J. TABOR, E. P. MAGRE and J. BOON, *Eur. Polym. J.* **7** (1971) 1127.
2. D. G. BRADY, *J. Appl. Polym. Sci.* **20** (1976) 2541.
3. A. J. LOVINGER, D. D. DAVIS and F. J. PADDEN, *Polymer* **26** (1985) 1595.
4. G. D. ANDREETTI, J. GARBARCZYK and M. KROLIKOWSKA, *Cryst. Struct. Commun.* **10** (1981) 789.
5. J. GARBARCZYK, *Makromol. Chem.* **187** (1986) 2489.
6. *Idem, Polym. Commun.* **27** (1986) 335.
7. N. T. WAKELYN, *J. Polym. Sci. Polym. Lett.* **25** (1987) 25.
8. J. N. HAY, J. I. LANGFORD and J. R. LLOYD, *Polymer* **30** (1989) 489.
9. J. S. CHUNG and P. CEBE, *ibid.* **33** (1992) 1594.
10. *Idem, J. Polym. Sci. Polym. Phys. Ed.* **30** (1992) 163.
11. P. CEBE and S. CHUNG, *Polym. Compos.* **11** (1990) 265.
12. A. D. Mighell and J. K. Stalick (eds), "Crystal Data: Determinative Tables", (US Department of Commerce, National Bureau of Standard and JCPDS-International Center for Diffraction Data, Swarthmore, PA, 1983).
13. P. HUO and P. CEBE, *Mater. Res. Soc. Symp. Proc.* **215** (1991) 93.
14. *Idem, J. Polym. Sci. Polym. Phys. Ed.* **30** (1992) 239.
15. S. Z. D. CHENG, B. CAO and B. WUNDERLICH, *Macromol.* **19** (1986) 1868.
16. P. HUO and P. CEBE, *Colloid. Polym. Sci.* (1992) in press.
17. N. S. MURTHY, R. L. ELSENBAUMER, J. E. FROMMER and R. H. BAUGHMAN, *Synth. Met.* **9** (1984) 91.
18. L. D'ILARIO and A. PIOZZI. *J. Mater. Sci. Lett.* **8** (1989) 157.
19. C. M. HSIUNG, M. CAKMAK and J. L. WHITE, *SPE ANTEC* **XXXII** (1986) 128.
20. E. MAEMURA, M. CAKMAK and J. L. WHITE, *Int. Polym. Proc.* **2** (1988) 79.
21. L. C. LOPÈZ and G. L. WILKES, *Polymer* **29** (1988) 106.
22. J. S. CHUNG and P. CEBE, *Polymer*, parts I and II (1992) in press.

Received 16 July 1991
and accepted 16 January 1992